

Energetics of Atmospherically Implicated Clusters Made of Sulfuric Acid, Ammonia, and Dimethyl Amine

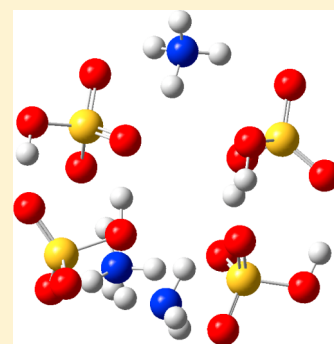
Hannah R. Leverentz,[†] J. Ilja Siepmann,^{*,†} Donald G. Truhlar,^{*,†} Ville Loukonen,[‡]
and Hanna Vehkamäki^{*,‡}

[†]Department of Chemistry, Chemical Theory Center, and Supercomputing Institute, University of Minnesota, Minneapolis, Minnesota 55455-0431, United States

[‡]Department of Physics, P.O. Box 64, University of Helsinki, 00014 Helsinki, Finland

S Supporting Information

ABSTRACT: The formation of atmospheric aerosol particles through clustering of condensable vapors is an important contributor to the overall concentration of these atmospheric particles. However, the details of the nucleation process are not yet well understood and are difficult to probe by experimental means. Computational chemistry is a powerful tool for gaining insights about the nucleation mechanism. Here, we report accurate electronic structure calculations of the potential energies of small clusters made from sulfuric acid, ammonia, and dimethylamine. We also assess and validate the accuracy of less expensive methods that might be used for the calculation of the binding energies of larger clusters for atmospheric modeling. The PW6B95-D3 density-functional-plus-molecular-mechanics calculation with the MG3S basis set stands out as yielding excellent accuracy while still being affordable for very large clusters.



1. INTRODUCTION

Radiative forcing associated with atmospheric aerosol particles is the largest source of uncertainty in global climate modeling.¹ A significant fraction of the overall atmospheric aerosol concentration is formed via gas-to-particle conversion. Although neither the chemical components involved nor the nucleation mechanisms for the formation of new particles have been unambiguously determined, there is convincing evidence that, in addition to water, sulfuric acid is involved in the formation of uncharged particles.² Because a binary mixture of water and sulfuric acid at relevant atmospheric concentrations is insufficient to explain the magnitude of observed nucleation rates and the large scatter between different observation sites, other chemical compounds have been implicated. Bases such as ammonia, amines, or aromatic nitrogen-containing heterocycles are the strongest candidates to contribute to the nucleation process; consequently, they have been the focus of recent experimental and computational investigations.^{3–7} The particle formation process can be clarified by computing formation free energies (relative to the monomers) for a range of cluster sizes and compositions. Furthermore, these free energies can be used to estimate the evaporation and fragmentation rates of the clusters. As these rates depend exponentially on the formation free energy differences, accurate potential energy surfaces are required. In the present study, the binding energies of clusters containing sulfuric acid and dimethylamine or sulfuric acid and ammonia are computed using a variety of electronic structure methods including wave function theory (WFT), density functional theory (DFT), and several multilevel methods, and we show that accurate calculations on large clusters are possible

by using approximate density functionals with post-self-consistent-field molecular mechanics terms.

2. SYSTEMS AND METHODS

Seven clusters were selected for this study. The clusters are called 1A1D, 2A1N, 2A2D, 3A2N, 3A3D, 4A3N, and 4A4D, where A denotes acid, in particular H₂SO₄, D denotes dimethylamine (DMA), and N denotes ammonia (NH₃); for example, 4A4D denotes a cluster composed of four acid molecules and four dimethyl amine molecules. These clusters are shown in Figure 1. Although each cluster has a neutral charge overall, notice that in many of the clusters a proton transfer has occurred so that often the clusters are actually composed partly of bisulfate ions and ammonium or dimethylammonium ions.

The geometries of the 1A1D cluster and the individual H₂SO₄ and DMA molecules used to calculate the 1A1D binding energy were optimized with the PW91 density functional⁸ and the 6-311++G(3df,3pd) basis set.⁹ The geometries of the remaining clusters and the H₂SO₄, DMA, and ammonia molecules used to calculate their binding energies were optimized with the B3LYP density functional¹⁰ and the CBSB7 basis set.¹¹

The initial structures for the geometry optimizations were obtained by a semiautomated conformational sampling procedure.⁵ In this procedure, a large set of cluster geometries (~10⁴) is first produced and, on the basis of simple criteria,

Received: March 7, 2013

Published: April 10, 2013

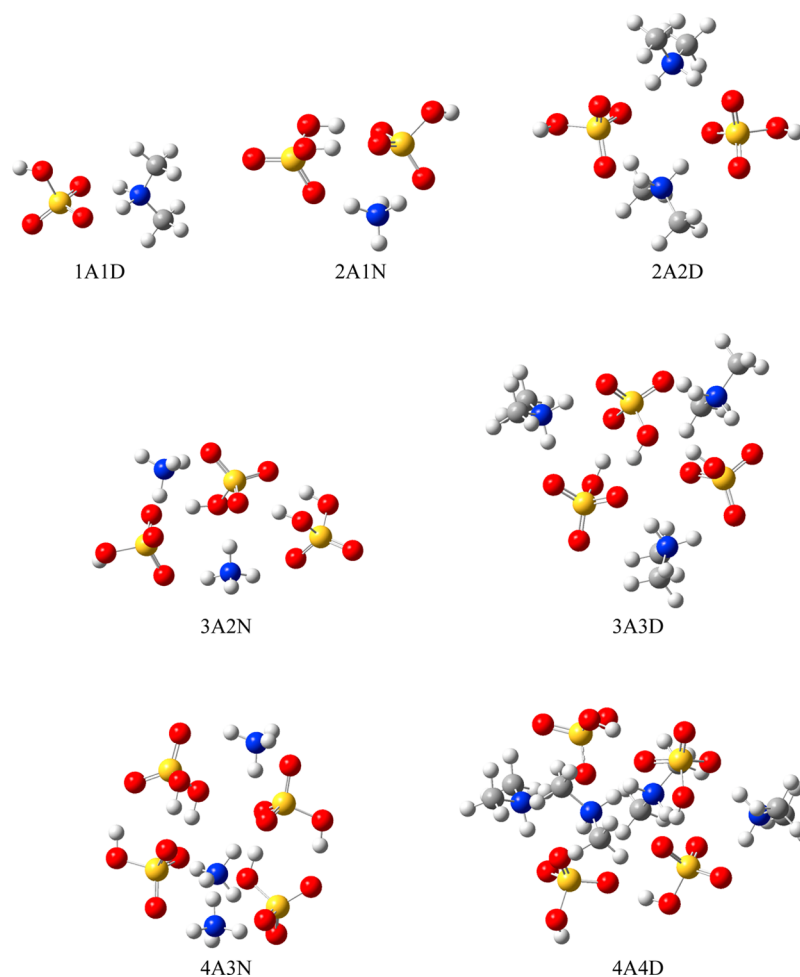


Figure 1. Clusters composed of sulfuric acid and ammonia or of sulfuric acid and dimethylamine.

about 50 distinct cluster structures are selected. These clusters are then optimized with lower-level methods (such as AM1,¹² PM3,¹³ or DFTB¹⁴). After the first optimization, the resulting clusters are inspected, and the most promising candidates are then optimized with the higher level of theory mentioned above. In general, finding global minimum energy structures is a nontrivial task, and it can be difficult to make sure that the relevant conformational space is thoroughly sampled.

Twenty-three methods were used to calculate the binding energies of the seven clusters, where a method is (1) a multilevel method, (2) a combination of a level of electronic structure wave function theory and a basis set, (3) a combination of a density functional and a basis set, or (4) a combination of a density functional, a basis set, and a molecular mechanics correction term. These methods were selected, on the basis of previous experience, as methods with good performance-to-price ratios. Six of these methods are based on wave function theory: CCSD(T)-F12a¹⁵ with the jun-cc-pV(T+d)Z,¹⁶ may-cc-pV(T+d)Z,¹⁶ aug-cc-pV(D+d)Z,¹⁷ jul-cc-pV(D+d)Z,¹⁶ and jun-cc-pV(D+d)Z¹⁶ basis sets and RI-CC2¹⁸ with the aug-cc-pV(T+d)Z¹⁷ basis set. Fourteen of the 23 methods are based on density functional theory (DFT) or a combination of density functional theory with a molecular mechanics correction term of the damped dispersion form (DFT-D). In all of the latter cases, the damped dispersion term is based on the D3¹⁹ method. The DFT and DFT-D calculations are based on the following approximate density functionals and basis sets:

B3LYP,¹⁰ B3LYP-D3, BLYP,^{20,21} BLYP-D3, M06-L,²² M06-L-D3, M11-L,²³ MN12-L,²⁴ PBE,²⁵ PBE-D3, PW6B95,²⁶ PW6B95-D3, and PW91⁸ each with the MG3S²⁷ basis set and M06-2X²² with the may-cc-pV(T+d)Z¹⁶ basis set. The remaining three methods are multilevel methods, where multilevel energies, sometimes called composite energies, are defined as linear combinations of electronic energies computed by two or more methods of electronic structure theory. In the multilevel methods used here, BMC-CCSD,²⁸ MCUT-TS,²⁹ and MCCO-TS,²⁹ higher-order correlation effects are computed with smaller basis sets so that the effects of expensive basis set extensions are estimated with less intrinsically costly levels of theory.

All CCSD(T)-F12a calculations and some components of the multilevel calculations on the larger clusters were done using Molpro 2010.1.³⁰ The core orbitals were frozen during all CCSD(T)-F12a calculations in accordance with the default settings of Molpro 2010.1. All RI-CC2 calculations were performed with Turbomole 6.4.³¹ All DFT calculations and the remaining components of the multilevel calculations on large clusters were carried out using Gaussian 09.³² Multilevel calculations on smaller clusters were performed using MLGAUSS 2.0.³³ The D3 energy contributions needed for the BLYP-D3, PBE-D3, and PW6B95-D3 calculations were calculated using DFT-D3, ver. 2.1 rev. 3, with damping to zero.^{21,34}

Table 1. Cluster Binding Energies^a and Mean Unsigned Deviations [kcal/(mol of Cluster)]

method	1A1D	2A1N	2A2D	3A2N	3A3D	4A3N	4A4D	MUD jnTZ ^b	MUD aDZ ^b
CCSD(T)-F12a/jun-cc-pV(T+d)Z	-24.54	-45.99	N/A	N/A	N/A	N/A	N/A	0.00	N/A
CCSD(T)-F12a/may-cc-pV(T+d)Z	-24.46	-46.41	N/A	N/A	N/A	N/A	N/A	0.25	N/A
CCSD(T)-F12a/aug-cc-pV(D+d)Z	-24.88	-46.77	-85.97	-95.61	N/A	N/A	N/A	0.56	0.00
CCSD(T)-F12a/jul-cc-pV(D+d)Z	-24.82	-46.87	-85.43	-95.71	N/A	N/A	N/A	0.58	0.20
CCSD(T)-F12a/jun-cc-pV(D+d)Z	-24.85	-47.61	-86.33	-97.46	N/A	N/A	N/A	0.96	0.77
PW6B95-D3/MG3S	-24.16	-45.82	-84.71	-93.46	-146.38	-146.55	-203.55	0.28	1.27
PBE-D3/MG3S	-26.16	-47.33	-87.26	-97.84	-151.30	-151.53	-210.02	1.48	1.34
BMC-CCSD	-25.01	-47.44	-88.76	-97.63	-154.74	-152.51	N/A	0.96	1.40
BLYP-D3/MG3S	-26.49	-45.76	-91.33	-95.69	-157.55	-148.19	-219.52	1.09	2.01
M06-2X/may-cc-pV(T+d)Z	-22.81	-46.03	-79.65	-92.42	-139.46	-143.23	-192.20	0.89	3.08
RI-CC2/aug-cc-pV(T+d)Z	-27.13	-48.44	-90.99	-99.64	-158.70	-155.46	-221.58	2.52	3.24
B3LYP-D3/MG3S	-26.81	-48.38	-92.27	-99.60	-159.94	-154.74	-222.92	2.33	3.46
PW91	-23.73	-44.11	-77.31	-89.73	-132.34	-137.59	-179.24	1.35	4.59
MCUT-TS	-22.76	-43.07	-79.94	-87.96	-137.02	-135.39	N/A	2.35	4.88
MCCO-TS	-23.11	-43.30	-79.30	-87.95	-135.79	-135.09	N/A	2.06	4.89
M06-L-D3/MG3S	-21.26	-43.30	-77.56	-90.23	-135.89	-140.15	-190.40	2.98	5.22
M06-L/MG3S	-20.89	-42.78	-75.66	-88.78	-132.33	-137.18	-183.63	3.43	6.28
PBE/MG3S	-22.76	-42.29	-74.58	-86.24	-127.28	-132.01	-172.28	2.74	6.84
PW6B95/MG3S	-21.47	-41.96	-75.19	-85.11	-128.75	-131.86	-176.10	3.55	7.37
MN12-L/MG3S	-18.71	-42.99	-71.10	-86.51	-125.03	-135.23	-171.73	4.41	8.48
B3LYP/MG3S	-21.08	-40.09	-72.28	-81.44	-122.49	-123.87	-165.72	4.68	9.58
M11-L/MG3S	-16.61	-39.88	-65.12	-82.10	-114.05	-126.48	-158.72	7.02	12.38
BLYP/MG3S	-19.64	-35.52	-66.70	-73.31	-111.58	-110.89	-149.88	7.68	14.52
<i>BMC-CCSD Components</i>									
CCSD/6-31BD	-29.02	-50.21	-98.84	-106.84	-168.19	-167.77	N/A	4.35	7.92
MP4DQ/6-31BD	-28.75	-49.82	-98.11	-106.01	-166.88	-166.43	N/A	4.02	7.36
MP2/MG3A	-26.06	-48.32	-90.05	-99.39	-156.16	-154.87	N/A	1.93	2.65
MP2/6-31BD	-31.33	-52.90	-102.89	-112.24	-175.86	-176.77	N/A	6.85	11.53
HF/MG3A	-16.59	-36.02	-68.18	-73.05	-113.58	-109.64	N/A	8.96	14.85
HF/6-31BD	-23.27	-43.72	-85.28	-91.91	-142.76	-141.68	N/A	1.77	2.26
<i>MCUT-TS Components</i>									
MP4(SDQ)/6-31G(d)	-25.29	-49.03	-89.83	-102.85	-154.82	-160.99	-217.15	1.89	3.44
MP2/MG3S	-26.00	-48.18	-89.70	-99.08	-155.48	-154.17	N/A	1.82	2.43
MP2/6-31+G(d,p)	-26.88	-48.35	-92.88	-101.91	-162.42	-161.21	-229.13	2.35	4.19
MP2/6-31G(d)	-27.75	-52.31	-94.62	-109.30	-163.52	-171.30	-228.65	4.76	7.69
TPSSKICIS(2)/MG3S	-21.89	-40.71	-73.54	-82.80	-124.36	-126.39	-168.23	3.97	8.57
HF/6-31G(d)	-19.54	-41.73	-75.93	-86.46	-128.18	-132.19	-177.86	4.63	7.39
<i>MCCO-TS Components</i>									
MP2/MG3S	-26.00	-48.18	-89.70	-99.08	-155.48	-154.17	N/A	1.82	2.43
MP2/6-31G(d)	-27.75	-52.31	-94.62	-109.30	-163.52	-171.30	-228.65	4.76	7.69
TPSSKICIS(1)/MG3S	-21.96	-41.58	-74.39	-84.23	-126.11	-128.57	-170.87	3.50	7.77
HF/6-31G(d)	-19.54	-41.73	-75.93	-86.46	-128.18	-132.19	-177.86	4.63	7.39

^aBinding energy = (energy of the cluster) – (sum of the monomer energies). All results are potential energy differences, i.e., they exclude vibrational and rotational contributions. ^bMUD jnTZ = the mean unsigned deviation from the CCSD(T)-F12a/jun-cc-pV(T+d)Z results for the 1A1D and 2A1N clusters. MUD aDZ = the mean unsigned deviation from the CCSD(T)-F12a/aug-cc-pV(D+d)Z results for the 1A1D, 2A1N, 2A2D, and 3A2N clusters.

3. RESULTS AND DISCUSSION

Table 1 shows the binding energy of each cluster calculated using each of the 23 methods. The second-to-last column of Table 1 shows for each method the mean unsigned deviation (MUD) for the two smallest clusters from what we believe to be the best method used in this study: CCSD(T)-F12a/jun-cc-pV(T+d)Z. The last column of Table 1 shows mean unsigned deviations for the four smallest clusters from CCSD(T)-F12a/aug-cc-pV(D+d)Z, which is the best method with which we were able to obtain data on a cluster containing three sulfuric acid molecules.

The 23 methods listed in Table 1 are shown in decreasing order of reliability according to the mean unsigned deviation

(MUD) from the CCSD(T)-F12a/aug-cc-pV(D+d)Z result for the four cases for which that result is available (see footnote b in the table). Comparing the final two columns of Table 1, we see that the conclusions about the relative accuracies of the methods are not strongly dependent on which error column we use. Therefore, we propose that a reasonably simple way to estimate the relative accuracies can be based on the mean unsigned deviation from a single best estimate (BE). For the 1A1D and 2A1N clusters, the best estimate is defined as the CCSD(T)-F12a/jun-cc-pV(T+d)Z binding energy. For the 2A2D and 3A2N clusters, the best estimate is the CCSD(T)-F12a/aug-cc-pV(D+d)Z binding energy scaled by a factor of 0.985. The scale factor of 0.985 was obtained by taking the

Table 2. Cluster Binding Energies^a and Mean Unsigned Deviations from the Best Estimates [kcal/(mol of Cluster)]

method	1A1D	2A1N	2A2D	3A2N	3A3D	4A3N	4A4D	MUD ^b
best estimate ^b	-24.54	-45.99	-84.68	-94.18	N/A	N/A	N/A	0.00
PW6B95-D3/MG3S	-24.16	-45.82	-84.71	-93.46	-146.38	-146.55	-203.55	0.32
M06-2X/may-cc-pV(T+d)Z	-22.81	-46.03	-79.65	-92.42	-139.46	-143.23	-192.20	2.14
PBE-D3/MG3S	-26.16	-47.33	-87.26	-97.84	-151.30	-151.53	-210.02	2.30
BMC-CCSD	-25.01	-47.44	-88.76	-97.63	-154.74	-152.51	N/A	2.36
BLYP-D3/MG3S	-26.49	-45.76	-91.33	-95.69	-157.55	-148.19	-219.52	2.58
PW91	-23.73	-44.11	-77.31	-89.73	-132.34	-137.59	-179.24	3.63
MCUT-TS	-22.76	-43.07	-79.94	-87.96	-137.02	-135.39	N/A	3.91
MCCO-TS	-23.11	-43.30	-79.30	-87.95	-135.79	-135.09	N/A	3.93
M06-L-D3/MG3S	-21.26	-43.30	-77.56	-90.23	-135.89	-140.15	-190.40	4.26
B3LYP-D3/MG3S	-26.81	-48.38	-92.27	-99.60	-159.94	-154.74	-222.92	4.42
M06-L/MG3S	-20.89	-42.78	-75.66	-88.78	-132.33	-137.18	-183.63	5.32
RI-CC2/aug-cc-pV(T+d)Z	-27.22	-49.12	-95.84	-100.67	-159.87	-155.46	-221.58	5.87
PBE/MG3S	-22.76	-42.29	-74.58	-86.24	-127.28	-132.01	-172.28	5.88
PW6B95/MG3S	-21.47	-41.96	-75.19	-85.11	-128.75	-131.86	-176.10	6.41
MN12-L/MG3S	-18.71	-42.99	-71.10	-86.51	-125.03	-135.23	-171.73	7.52
B3LYP/MG3S	-21.08	-40.09	-72.28	-81.44	-122.49	-123.87	-165.72	8.62
M11-L/MG3S	-16.61	-39.88	-65.12	-82.10	-114.05	-126.48	-158.72	11.42
BLYP/MG3S	-19.64	-35.52	-66.70	-73.31	-111.58	-110.89	-149.88	13.56

^aBinding energy = (energy of the cluster) - (sum of the monomer energies). All results are potential energy differences, i.e., they exclude vibrational and rotational contributions. ^bMean unsigned deviation with respect to best estimate, which is specified in the text. The average is taken over the 1A1D, 2A1N, 2A2D, and 3A2N clusters.

Table 3. Relative Computational Cost^a (Unitless) of a Single-Point Energy Calculation

method	1A1D	2A1N	2A2D	3A2N	3A3D	4A3N	4A4D
CCSD(T)-F12a/jun-cc-pV(T+d)Z	205	1922	^b	^b	^b	^b	^b
CCSD(T)-F12a/may-cc-pV(T+d)Z	325	1335	^b	^b	^b	^b	^b
CCSD(T)-F12a/aug-cc-pV(D+d)Z	87	351	3432	3612	^b	^b	^b
CCSD(T)-F12a/jul-cc-pV(D+d)Z	31	203	3040	3314	^b	^b	^b
CCSD(T)-F12a/jun-cc-pV(D+d)Z	19	77	1718	1745	^b	^b	^b
B3LYP/MG3S	2	4	15	14	46	36	93
B3LYP-D3/MG3S	2	4	15	14	46	36	93
BLYP/MG3S	1	2	7	6	18	14	32
BLYP-D3/MG3S	1	2	7	6	18	14	32
BMC-CCSD	3	11	91	114	2390	1477	^b
M06-2X/may-cc-pV(T+d)Z	3	6	24	20	82	52	159
M06-L/MG3S	2	3	9	9	24	18	46
M06-L-D3/MG3S	2	3	9	9	24	18	46
M11-L/MG3S	1	2	4	4	10	9	22
MCCO-TS	5	12	63	68	651	^c	^b
MCUT-TS	5	14	108	114	^c	635	^b
MN12-L/MG3S	2	3	9	9	24	19	54
PBE/MG3S	2	2	7	6	18	14	32
PBE-D3/MG3S	2	2	7	6	18	14	32
PW6B95-D3/MG3S	3	5	16	30	32	18	52
PW6B95/MG3S	3	5	16	30	32	18	52
PW91/MG3S	1	2	7	6	18	14	32
RI-CC2/aug-cc-pV(T+d)Z	7	12	59	60	368	205	1055

^aRelative to the cost of the M11-L/MG3S single-point energy calculation on the 1A1D cluster. See text for a more complete description of how these values were obtained. ^bThese calculations were not completed because they required more than the maximum amount of memory per processor than that which was available to us. ^cThe timing information for this calculation is not available.

average of the ratios of the CCSD(T)-F12a/jun-cc-pV(T+d)Z binding energy to the CCSD(T)-F12a/aug-cc-pV(D+d)Z over the two clusters (1A1D and 2A1N) where binding energies calculated at both the CCSD(T)-F12a/jun-cc-pV(T+d)Z and the CCSD(T)-F12a/aug-cc-pV(D+d)Z levels were available.

Table 2 shows, for the four smallest clusters, the mean unsigned deviation (MUD) from the best estimates. This table indicates that the PW6B95-D3 functional with the MG3S basis

set is an excellent way to obtain accurate binding energies (with a MUD of less than 0.5 kcal/mol for the test set) for larger clusters of sulfuric acid with DMA or ammonia. The MUD for the PW6B95/MG3S method (i.e., without the molecular mechanics term) is much larger. Furthermore, all other methods investigated here yield MUD values greater than 2 kcal/mol, and such large errors would likely lead to significant errors in the estimation of cluster formation free energies.

To decide what method has the best performance for a given cost, we estimated the computational costs of the various calculations on the basis of the computer time required to carry out each calculation (this estimate therefore neglects the cost of computer memory, but it is sufficient for our purposes). Because the calculations were performed on different machines and with different software programs, all costs are expressed in reduced units (r.u.). For a given calculation, performed with software package *S* on a given processor, one r.u. is the computer time for an MP2/MG3S single-point energy calculation of the 1A1D cluster with software *S* on that same processor. (For composite methods, we first compute the cost of each component in r.u., and then we add those costs.) Table 3 shows the relative computational cost of all the single-point energy calculations; the relative cost is defined as the cost in r.u. divided by the cost in r.u. for the least expensive calculation (which is the M11-L/MG3S calculation on 1A1D).

To determine which method has the best performance for a given cost, in Figure 2 we plot the MUD from the best estimate

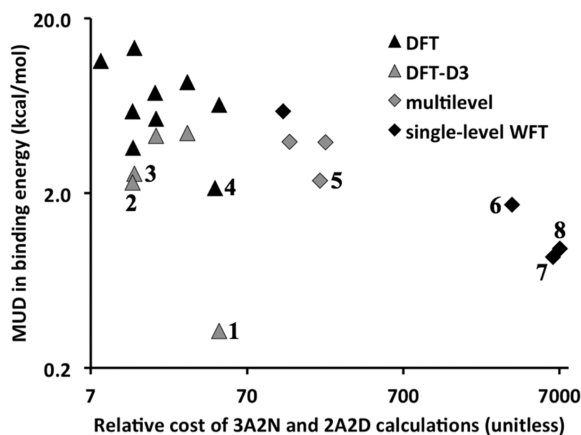


Figure 2. The mean unsigned deviation (MUD) in binding energies over the four smallest clusters plotted against the sum of the relative costs (unitless) of single-point energy calculations on the 2A2D and 3A2N clusters for various electronic structure methods. Labels on data points: (1) PW6B95-D3/MG3S, (2) PBE-D3/MG3S, (3) BLYP-D3/MG3S, (4) M06-2X/may-cc-pV(T+d)Z, (5) BMC-CCSD, (6) CCSD(T)-F12a/jun-cc-pV(D+d)Z, (7) CCSD(T)-F12a/jul-cc-pV(D+d)Z, (8) CCSD(T)-F12a/aug-cc-pV(D+d)Z.

values over the four smallest clusters (1A1D, 2A1N, 2A2D, and 3A2N) against the sum of the relative costs of single-point energy calculations on the 2A2D and 3A2N clusters for all DFT, DFT-D, and multilevel methods as well as the three single-level WFT methods for which data on all four clusters are available. Methods with the best performance-to-cost ratios are labeled in Figure 2. Data point 1 corresponds to PW6B95-D3/MG3S, which has the lowest MUD. Data points 2 and 3 correspond to DFT-D methods PBE-D3/MG3S and BLYP-D3/MG3S, respectively. Data point 4 corresponds to DFT method M06-2X/may-cc-pV(T+d)Z, data point 5 is the multilevel method BMC-CCSD, and data points 6–8 are the single-level WFT methods CCSD(T)-F12a with the jun-, jul-, and aug-cc-pV(D+d)Z basis sets, respectively.

The conclusion that we draw from Figure 2 is that the PW6B95-D3 density functional with the MG3S basis set gives the best performance of all the methods tested and at a dramatically low relative cost. Detailed consideration of Tables 2 and 3 and Figure 2 leads to the conclusion that the PBE-D3

and BLYP-D3 functionals with the MG3S basis set and the M06-2X functional with the may-cc-pV(T+d)Z basis set are also very efficient methods for relatively accurate binding energy calculations of sulfuric acid–DMA and sulfuric acid–ammonia clusters. Three of these four methods involve molecular mechanics terms, but if we limit ourselves to methods that do not involve molecular mechanics terms (because they are more likely to be trustworthy for general systems without additional validation), the best methods (on an accuracy for a given cost basis), in addition to M06-2X/may-cc-pV(T+d)Z, are BMC-CCSD and CCSD(T)-F12a with jun-cc-pV(D+d)Z or jul-cc-pV(D+d)Z.

It is encouraging that the electronic structure methods with the best cost–performance ratios are methods that have also been singled out for good performance in previous work in other contexts; this gives us confidence that they are not just performing well because of a fortuitous cancellation of errors. For example, the addition of the D3 damped dispersion correction consistently improves the performance of a variety of popular density functionals for the study of noncovalently interacting systems,³⁵ and the PW6B95-D3 density functional was singled out for especially good performance in three studies by Grimme and co-workers,^{36–38} and the M06-2X functional has shown good performance on a large number of problems.^{22,39–41} The BMC-CCSD method has previously been shown to have excellent performance for hydrogen bonding,⁴² and the CCSD(T)-F12a/jun-cc-pV(D+d)Z method showed very good performance for reaction energies and barrier heights.⁴³ We therefore have added confidence in our recommendation of these methods for future studies of atmospheric aerosol formation.

4. CONCLUSIONS

In this work, we have used a wide range of electronic structure methods to compute the binding energies of seven clusters composed of sulfuric acid and ammonia or dimethylamine, molecules which are believed to be important components in the precursor clusters of atmospheric aerosols. The goals of this work were to (1) obtain benchmark binding energies of relatively large atmospherically relevant clusters at the highest level of electronic structure theory affordable for these systems and (2) to determine which lower-cost electronic structure methods give the best balance between computational cost and energetic accuracy for these types of clusters and therefore can be recommended for use in future studies of atmospheric aerosol formation.

In fulfillment of the first goal, we obtained benchmark binding energies of clusters containing up to two sulfuric acid molecules and one ammonia molecule (11 heavy atoms) with CCSD(T)-F12a/jun-cc-pV(T+d)Z. We also obtained benchmark binding energies of clusters containing up to three sulfuric acid molecules and two ammonia molecules (17 heavy atoms) with CCSD(T)-F12a/aug-cc-pV(D+d)Z. In fulfillment of the second goal, we performed the same binding energy calculations with a wide range of electronic structure methods, including additional wave function theory methods with smaller basis sets, density functional methods both with and without molecular mechanics corrections, and multilevel methods, and we compared them to the benchmark results. We found that the method that gives the most accurate results relative to our best estimates of the binding energies is also one of the most computationally affordable methods: the PW6B95-D3 density functional with the MG3S basis set. We found that the other

two density functional methods tested in this study that include damped dispersion corrections, PBE-D3 and BLYP-D3 with the MG3S basis set, also give a good ratio of accuracy to cost, as does the M06-2X density functional with the may-cc-pV(T+d)Z basis set. These findings are in good agreement with expectations on the basis of a wide variety of previous studies.^{22,35–41} With the best balance of cost and accuracy overall, we recommend the PW6B95-D3 density functional with the MG3S basis set for future studies of atmospheric cluster formation.

■ ASSOCIATED CONTENT

■ Supporting Information

Tables of the Cartesian coordinates of the molecules and clusters. This material is available free of charge via the Internet at <http://pubs.acs.org>.

■ AUTHOR INFORMATION

Corresponding Author

*E-mail: siepmann@umn.edu (J.I.S.), truhlar@umn.edu (D.G.T.), hanna.vehkamaki@helsinki.fi (H.V.).

Notes

The authors declare no competing financial interest.

■ ACKNOWLEDGMENTS

Financial support from the National Science Foundation (CHE-1051396), Maj and Tor Nessling Foundation (project #2011200), the Academy of Finland (Center of Excellence program project #1118615, LASTU program project #135054), and the European Research Council (project ERC-StG 257360-MOCAPAF) is gratefully acknowledged. A portion of this research was performed using EMSL, a national scientific user facility sponsored by the Department of Energy's Office of Biological and Environmental Research and located at Pacific Northwest National Laboratory. Other portions of this research were performed using the high-performance computing resources at the Minnesota Supercomputing Institute.

■ REFERENCES

- (1) *The Intergovernmental Panel on Climate Change: Climate Change 2007: The Physical Science Basis*; Cambridge University Press: New York, 2007.
- (2) Kuang, C.; McMurry, P. H.; McCormick, A. V.; Eisele, F. L. Dependence of nucleation rates on sulfuric acid vapor concentration in diverse atmospheric locations. *J. Geophys. Res.* **2008**, *113*, D10209.
- (3) Chen, M.; Titcombe, M.; Jiang, J.-K.; Jen, C.; Kuang, C.-G.; Fischer, M. L.; Eisele, F. L.; Siepmann, J. I.; Hanson, D. R.; Zhao, J.; McMurry, P. H. Acid-base chemical reaction model for nucleation rates in the polluted atmospheric boundary layer. *Proc. Natl. Acad. Sci. U.S.A.* **2012**, *109*, 18713–18718.
- (4) Anderson, K. E.; Siepmann, J. I.; McMurry, P. H.; VandeVondele, J. Importance of the number of acid molecules and the strength of the base for double-ion formation in $(\text{H}_2\text{SO}_4)_m$ -base- $(\text{H}_2\text{O})_6$ clusters. *J. Am. Chem. Soc.* **2008**, *130*, 14144–14147.
- (5) Ortega, I. K.; Kupiainen, O.; Kurtén, T.; Olenius, T.; Wilkman, O.; McGrath, M. J.; Loukonen, V.; Vehkamäki, H. From quantum chemical formation free energies to evaporation rates. *Atmos. Chem. Phys.* **2012**, *12*, 225–235.
- (6) Liu, W.-W.; W.; X.-L.; Chen, S.-L.; Zhang, Y.-H.; Li, Z.-S. Theoretical study on reaction mechanism of sulfuric acid and ammonia and hydration of $(\text{NH}_4)_2\text{SO}_4$. *Theor. Chem. Acc.* **2012**, *131*, 1103.
- (7) Elm, J.; Bilde, M.; Mikkelsen, K. V. Assessment of Density Functional Theory in Predicting Structures and Free Energies of Reaction in Atmospheric Prenucleation Clusters. *J. Chem. Theory Comput.* **2012**, *8*, 2071–2077.

- (8) Perdew, J. P. In *Electronic Structure of Solids '91*; Ziesche, P., Eschrig, H., Eds.; Akademie Verlag: Berlin, 1991; p 11.

- (9) Frisch, M. J.; Pople, J. A.; Binkley, J. S. Self-consistent molecular-orbital methods. 25. Supplementary functions for Gaussian basis sets. *J. Chem. Phys.* **1984**, *80*, 3265–3269.

- (10) Becke, A. D. Density-functional exchange-energy approximation with correct asymptotic behavior. *Phys. Rev. A* **1988**, *38*, 3098–3100.

- (11) Montgomery, J. A., Jr.; Frisch, M. J.; Ochterski, J. W.; Petersson, G. A. A complete basis set model chemistry. VI. Use of density functional geometries and frequencies. *J. Chem. Phys.* **1999**, *110*, 2822–2827.

- (12) Dewar, M. J. S.; Zoebisch, E. G.; Healy, E. F.; Stewart, J. J. P. Development and use of quantum mechanical molecular models. 76. AM1: a new general purpose quantum mechanical molecular model. *J. Am. Chem. Soc.* **1985**, *107*, 3902–3909.

- (13) Stewart, J. J. P. Optimization of parameters for semiempirical methods I. Method. *J. Comput. Chem.* **1989**, *10*, 209.

- (14) Foulkes, W. M. C.; Haydock, R. Tight-binding models and density-functional theory. *Phys. Rev. B* **1989**, *39*, 12520–12536.

- (15) Knizia, G.; Adler, T. B.; Werner, H.-J. Simplified CCSD(T)-F12 methods: Theory and benchmarks. *J. Chem. Phys.* **2009**, *130*, 054104.

- (16) Papajak, E.; Truhlar, D. G. Convergent Partially Augmented Basis Sets for Post-Hartree-Fock Calculations of Molecular Properties and Reaction Barrier Heights. *J. Chem. Theory Comput.* **2011**, *7*, 10–18.

- (17) Dunning, T. H., Jr.; Peterson, K. A.; Wilson, A. K. Gaussian basis sets for use in correlated molecular calculations. X. The atoms aluminum through argon revisited. *J. Chem. Phys.* **2001**, *114*, 9244–9253.

- (18) Hättig, C.; Weigend, F. CC2 excitation energy calculations on large molecules using the resolution of the identity approximation. *J. Chem. Phys.* **2000**, *113*, 5154–5161.

- (19) Grimme, S.; Antony, J.; Ehrlich, S.; Krieg, H. A consistent and accurate ab initio parametrization of density functional dispersion correction (DFT-D) for the 94 elements H-Pu. *J. Chem. Phys.* **2010**, *132*, 154104.

- (20) Becke, A. D. Density-functional exchange-energy approximation with correct asymptotic behavior. *Phys. Rev. A* **1988**, *38*, 3098–3100.

- (21) Lee, C.; Yang, W.; Parr, R. G. Development of the Colle-Salvetti correlation-energy formula into a functional of the electron density. *Phys. Rev. B* **1988**, *37*, 785–789.

- (22) Zhao, Y.; Truhlar, D. G. The M06 suite of density functionals for main group thermochemistry, thermochemical kinetics, non-covalent interactions, excited states, and transition elements: two new functionals and systematic testing of four M06-class functionals and 12 other functionals. *Theor. Chem. Acc.* **2008**, *120*, 215–241.

- (23) Peverati, R.; Truhlar, D. G. M11-L: A Local Density Functional That Provides Improved Accuracy for Electronic Structure Calculations in Chemistry and Physics. *J. Phys. Chem. Lett.* **2012**, *3*, 117–124.

- (24) Peverati, R.; Truhlar, D. G. An improved and broadly accurate local approximation to the exchange–correlation density functional: The MN12-L functional for electronic structure calculations in chemistry and physics. *Phys. Chem. Chem. Phys.* **2012**, *14*, 13171–13174.

- (25) Perdew, J. P.; Burke, K.; Ernzerhof, M. Generalized Gradient Approximation Made Simple. *Phys. Rev. Lett.* **1996**, *77*, 3865–3868.

- (26) Zhao, Y.; Truhlar, D. G. Design of density functionals that are broadly accurate for thermochemistry, thermochemical kinetics, and nonbonded interactions. *J. Phys. Chem. A* **2005**, *109*, 5656–5667.

- (27) Lynch, B. J.; Zhao, Y.; Truhlar, D. G. Effectiveness of diffuse basis functions for calculating relative energies by density functional theory. *J. Phys. Chem. A* **2003**, *107*, 1384–1388.

- (28) Lynch, B. J.; Zhao, Y.; Truhlar, D. G. The 6-31B(d) basis set and the BMC-QCISD and BMC-CCSD multicoefficient correlation methods. *J. Phys. Chem. A* **2005**, *109*, 1643–1649.

- (29) Zhao, Y.; Lynch, B. J.; Truhlar, D. G. Multi-coefficient extrapolated density functional theory for thermochemistry and thermochemical kinetics. *Phys. Chem. Chem. Phys.* **2005**, *7*, 43–52.

(30) Werner, H.-J.; Knowles, P. J.; Knizia, G.; Manby, F. R.; Schütz, M.; Celani, P.; Korona, T.; Lindh, R.; Mitrushekov, A.; Rauhut, G.; Shamasundar, K. R.; Adler, T. B.; Amos, R. D.; Bernhardsson, A.; Berning, A.; Cooper, D. L.; Deegan, M. J. O.; Dobbyn, A. J.; Eckert, F.; Goll, E.; Hampel, C.; Hesselmann, A.; Hetzer, G.; Hrenar, T.; Jansen, G.; Köppl, C.; Liu, Y.; Lloyd, A. W.; Mata, R. A.; May, A. J.; McNicholas, S. J.; Meyer, W.; Mura, M. E.; Nicklass, A.; O'Neill, D. P.; Palmieri, P.; Pflüger, K.; Pitzer, R.; Reiher, M.; Shiozaki, T.; Stoll, H.; Stone, A. J.; Tarroni, R.; Thorsteinsson, T.; Wang, M.; Wolf, A. *MOLPRO*, version 2010.1, a package of ab initio programs; see <http://www.molpro.net>.

(31) *TURBOMOLE*, V6.4 2012, a development of University of Karlsruhe and Forschungszentrum Karlsruhe GmbH, 1989–2007, *TURBOMOLE* GmbH, since 2007; available from <http://www.turbomole.com>.

(32) Frisch, M. J.; Trucks, G. W.; Schlegel, H. B.; Scuseria, G. E.; Robb, M. A.; Cheeseman, J. R.; Scalmani, G.; Barone, V.; Mennucci, B.; Petersson, G. A.; Nakatsuji, H.; Caricato, M.; Li, X.; Hratchian, H. P.; Izmaylov, A. F.; Bloino, J.; Zheng, G.; Sonnenberg, J. L.; Hada, M.; Ehara, M.; Toyota, K.; Fukuda, R.; Hasegawa, J.; Ishida, M.; Nakajima, T.; Honda, Y.; Kitao, O.; Nakai, H.; Vreven, T.; Montgomery, J. A., Jr.; Peralta, J. E.; Ogliaro, F.; Bearpark, M.; Heyd, J. J.; Brothers, E.; Kudin, K. N.; Staroverov, V. N.; Kobayashi, R.; Normand, J.; Raghavachari, K.; Rendell, A.; Burant, J. C.; Iyengar, S. S.; Tomasi, J.; Cossi, M.; Rega, N.; Millam, N. J.; Klene, M.; Knox, J. E.; Cross, J. B.; Bakken, V.; Adamo, C.; Jaramillo, J.; Gomperts, R.; Stratmann, R. E.; Yazyev, O.; Austin, A. J.; Cammi, R.; Pomelli, C.; Ochterski, J. W.; Martin, R. L.; Morokuma, K.; Zakrzewski, V. G.; Voth, G. A.; Salvador, P.; Dannenberg, J. J.; Dapprich, S.; Daniels, A. D.; Farkas, Ö.; Foresman, J. B.; Ortiz, J. V.; Cioslowski, J.; Fox, D. J. *Gaussian 09*, version c01; Gaussian Inc.: Wallingford, CT, 2009.

(33) Zhao, Y.; Truhlar, D. G. *MLGAUSS*, version 2.0; University of Minnesota: Minneapolis, MN, 2006.

(34) Grimme, S.; Antony, J.; Ehrlich, S.; Krieg, H. *DFT-D3*, ver. 2.1 rev. 3; University of Münster: Münster, Germany, 2011; <http://toc.uni-muenster.de/DFTD3> (accessed August 6, 2012).

(35) Grimme, S. Density functional theory with London dispersion corrections. *WIREs Comput. Mol. Sci.* **2011**, *1*, 211–228.

(36) Goerigk, L.; Grimme, S. A thorough benchmark of density functional methods for general main group thermochemistry, kinetics, and noncovalent interactions. *Phys. Chem. Chem. Phys.* **2011**, *13*, 6670–6688.

(37) Goerigk, L.; Kruse, H.; Grimme, S. Benchmarking density functional methods against the S66 and S66x8 datasets for non-covalent interactions. *ChemPhysChem* **2011**, *12*, 3421–3433.

(38) Grimme, S.; Mück-Lichtenfeld, C. Accurate computation of structures and strain energies of cyclophanes with modern DFT methods. *Israel J. Chem.* **2012**, *52*, 180–192.

(39) Zhao, Y.; Truhlar, D. G. How well can new-generation density functionals describe the energetics of bond-dissociation reactions producing radicals? *J. Phys. Chem. A* **2008**, *112*, 1095–1099.

(40) Korth, M.; Grimme, S. Mindless DFT benchmarking. *J. Chem. Theory Comput.* **2009**, *5*, 993–1003.

(41) Zhao, Y.; Truhlar, D. G. Applications and Validations of the Minnesota Density Functionals. *Chem. Phys. Lett.* **2011**, *502*, 1–13.

(42) Zhao, Y.; Truhlar, D. G. Assessment of Model Chemistries for Noncovalent Interactions. *J. Chem. Theory Comput.* **2006**, *2*, 1009–1018.

(43) Papajak, E.; Truhlar, D. G. What are the Most Efficient Basis Set Strategies for Correlated Wave Function Calculations of Reaction Energies and Barrier Heights? *J. Chem. Phys.* **2012**, *137*, 064110.